

# Highly Crystalline, Idiomorphic $\text{Na}_2\text{Ti}_6\text{O}_{13}$ Whiskers Grown from a NaCl Flux at a Relatively Low Temperature

Katsuya Teshima,<sup>\*,[a]</sup> SunHyung Lee,<sup>[b]</sup> Serika Murakoshi,<sup>[a]</sup> Sayaka Suzuki,<sup>[a]</sup> Kunio Yubuta,<sup>[c]</sup> Toetsu Shishido,<sup>[c]</sup> Morinobu Endo,<sup>[d,e]</sup> and Shuji Oishi<sup>[a,d]</sup>

**Keywords:** Crystal growth / Photochemistry / Titanates / Photocatalysis

Well-developed, highly crystalline  $\text{Na}_2\text{Ti}_6\text{O}_{13}$  whiskers were successfully grown by cooling a NaCl flux at a relatively low temperature of 700 °C. The obtained  $\text{Na}_2\text{Ti}_6\text{O}_{13}$  whiskers were colorless and transparent. The whiskers grown at 700 °C were single phase and exhibit the lowest sizes of up to about  $3.5\ \mu\text{m} \times 0.1\ \mu\text{m}$ . From the results of SEM, XRD, and TEM, it was confirmed that the  $\text{Na}_2\text{Ti}_6\text{O}_{13}$  whiskers have

very good crystallinity and elongated in the  $\langle 010 \rangle$  directions. Furthermore, the whiskers exhibited good photocatalytic activity under ultraviolet light irradiation. It is reasonable to suppose that NaCl can be adequately used to synthesize high quality and well-developed titanate whiskers in an environmentally friendly process of crystal growth.

## Introduction

One-dimensional (1D) structural materials, such as, tubes, fibers, rods, whiskers, and belts, are expected to find many potential applications due to their novel chemical and physical properties in comparison to bulk materials.<sup>[1–10]</sup> In particular, 1D structures have attracted extraordinary attention as photocatalysts because they have a large specific surface area; however, uniformity, small sizes, and high crystallinity are required to maximize photocatalytic characteristics.<sup>[3–7,9]</sup> Recently, various 1D metal oxide compounds (such as tungstates, molybdates, niobates, tantalates, and titanates) were synthesized to be high potential photocatalysts.<sup>[2–6,9,11–13]</sup> Among them, sodium hexatitanate ( $\text{Na}_2\text{Ti}_6\text{O}_{13}$ ) crystal has been studied as a photocatalyst for the degradation of toxic substances and the decomposition of pure water and as oxygen electrodes in potentiometric sensors for  $\text{O}_2$  and  $\text{CO}_2$ .<sup>[14,15]</sup> In addition,  $\text{Na}_2\text{Ti}_6\text{O}_{13}$  forms the whisker structure, which is a needle-shaped single crystal with near theoretical strength due to its perfect geometry. The  $\text{Na}_2\text{Ti}_6\text{O}_{13}$  crystals have a unique tunnel structure

that consists of three vacant spaces, one of which corresponds to the removal of a  $\text{TiO}_6$  unit (Figure 1a). The  $\text{Na}_2\text{Ti}_6\text{O}_{13}$  whiskers have the same tunnel structure.<sup>[4]</sup>

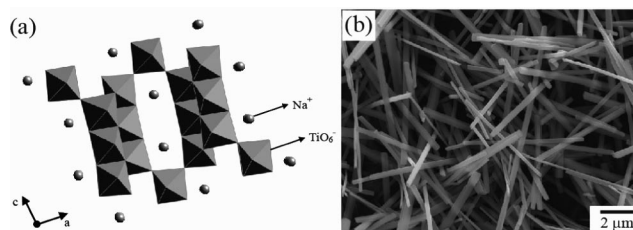


Figure 1. (a) Schematic representation of the  $\text{Na}_2\text{Ti}_6\text{O}_{13}$  structure; (b) SEM image of typical  $\text{Na}_2\text{Ti}_6\text{O}_{13}$  whiskers grown at 1100 °C (Run 1) using a cooling method with a NaCl flux.

The  $\text{Na}_2\text{Ti}_6\text{O}_{13}$  crystal is monoclinic with the  $C2/m$  space group.  $\text{Na}_2\text{Ti}_6\text{O}_{13}$  has lattice parameters of  $a = 1.512\ \text{nm}$ ,  $b = 0.374\ \text{nm}$ ,  $c = 0.916\ \text{nm}$ , and  $\beta = 99.3^\circ$ .<sup>[16]</sup> The melting point of  $\text{Na}_2\text{Ti}_6\text{O}_{13}$  is 1300 °C. We first reported on the growth of highly uniform, crystalline, and hexagonal prismatic  $\text{Na}_2\text{Ti}_6\text{O}_{13}$  whiskers with aspect ratios of up to 50 by the slow cooling of a NaCl flux.<sup>[4]</sup> Recently, we successfully downsized the  $\text{Na}_2\text{Ti}_6\text{O}_{13}$  whiskers to  $101.5\ \mu\text{m} \times 0.7\ \mu\text{m}$  in average size (a high aspect ratio of 145) by controlling the cooling rate.<sup>[3]</sup> Typical as-grown  $\text{Na}_2\text{Ti}_6\text{O}_{13}$  whiskers are shown in Figure 1b. The  $\text{Na}_2\text{Ti}_6\text{O}_{13}$  whiskers demonstrated good photocatalytic activity under ultraviolet (UV) light irradiation; however, the  $\text{Na}_2\text{Ti}_6\text{O}_{13}$  whiskers were grown at a relatively high holding temperature of 1100 °C. The melting point of NaCl (801 °C) is relatively low. Here, we report on the fabrication of  $\text{Na}_2\text{Ti}_6\text{O}_{13}$  whiskers at a relatively low temperature ( $<1100\ ^\circ\text{C}$ ) by the cooling of a NaCl flux.

[a] Department of Environmental Science and Technology, Faculty of Engineering, Shinshu University, Nagano 380-8553, Japan  
Fax: +81-26-269-5550  
E-mail: teshima@shinshu-u.ac.jp

[b] Faculty of Engineering, Shinshu University, Nagano 380-8553, Japan

[c] Institute for Materials Research, Tohoku University, Sendai 980-8577, Japan

[d] Institute of Carbon Science and Technology, Shinshu University, Nagano 380-8553, Japan

[e] Department of Electrical and Electronic Engineering, Faculty of Engineering, Shinshu University, Nagano 380-8553, Japan

Supporting information for this article is available on the WWW under <http://dx.doi.org/10.1002/ejic.200901175>.

Furthermore, the effects of the holding temperature, solute concentration, and cooling rate on the downsizing of the  $\text{Na}_2\text{Ti}_6\text{O}_{13}$  whiskers were studied.

## Results and Discussion

In this study, well-developed and uniform  $\text{Na}_2\text{Ti}_6\text{O}_{13}$  whiskers were successfully grown as a single phase by cooling a NaCl flux at relatively low temperatures of 700 to 1000 °C. The grown  $\text{Na}_2\text{Ti}_6\text{O}_{13}$  whiskers were idiomorphic and colorless-transparent. First, the effect of holding temperature on the growth and shape of the  $\text{Na}_2\text{Ti}_6\text{O}_{13}$  crystals was investigated. The holding temperature was varied from 600 to 1000 °C. The solute concentration and cooling rate were fixed at 0.5 mol-% and 5 °C h<sup>-1</sup>, respectively. Figure 2 depicts FESEM images of the crystals grown at various holding temperatures. When the holding temperature was in the range from 700 to 1000 °C, idiomorphic whiskers with a relatively high average aspect ratio were observed, as shown in Figure 2a,b. In comparison to our previous study (crystals grown at 1100 °C), well-developed, idiomorphic whiskers can be successfully grown herein at a much lower temperature (700 °C). Furthermore, when no NaCl was used (i.e., solid-state reaction), not idiomorphic whiskers, but large aggregates consisting of many nanoparticles were obtained, as clearly shown in the Supporting Information. In addition, the basic form of the whiskers consisted of a hexagonal cylinder, and their surfaces were very flat (Figure 2d). In contrast, 1D and bulk-like structures coexisted in the crystal grown at 600 °C (Run 6), as shown in Figure 2c. These bulk-like structures were thought to be  $\text{TiO}_2$  because the raw material (i.e., reagent-grade  $\text{TiO}_2$ ) was not completely melted at such a low temperature and the unreacted raw material remained due to a slow reaction rate. The average length, width, and aspect ratio of idiomorphic whiskers are summarized in Table 1. The length and width of the whiskers linearly increased in proportion to the holding temperature, as summarized in Table 1. Therefore, whisker size can be easily controlled by the holding temperature.

Figure 3a–c shows XRD profiles of the crystals grown at various holding temperatures. Figure 3d,e shows XRD profiles of the  $\text{Na}_2\text{Ti}_6\text{O}_{13}$  ICDD-PDF<sup>[16]</sup> and  $\text{TiO}_2$  ICDD-PDF<sup>[17]</sup>. When the holding temperature was in the range from 700 to 1000 °C, the resultant whiskers can be identified as  $\text{Na}_2\text{Ti}_6\text{O}_{13}$  by their powder XRD patterns in Figure 3a,b and by using data from the literature in Figure 3d. Diffraction patterns attributable to byproducts were not observed in Figure 3a,b. The XRD pattern for oriented whiskers indicates that the diffraction intensities of the (200), ( $\bar{2}$ 01), ( $\bar{2}$ 03), (402), ( $\bar{6}$ 01), ( $\bar{4}$ 04), and (602) planes were dominant (not shown in this paper). In contrast, crystals grown at 600 °C were observed to coexist with  $\text{Na}_2\text{Ti}_6\text{O}_{13}$  and  $\text{TiO}_2$ , as depicted in Figure 3c, by using data from the literature in Figure 3d,e. Because the grown whiskers (1D materials) were identified as  $\text{Na}_2\text{Ti}_6\text{O}_{13}$ , the bulk-like structure shown in Figure 2c is confirmed to be  $\text{TiO}_2$  (byproduct or unreacted raw material). From these FESEM and XRD

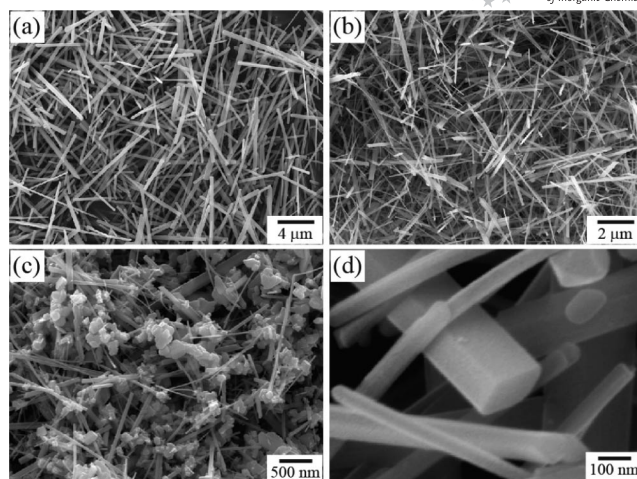


Figure 2. SEM images of products grown at (a) 1000 °C (Run 2), (b) 700 °C (Run 5), and (c) 600 °C (Run 6); (d) high-magnification image of typical  $\text{Na}_2\text{Ti}_6\text{O}_{13}$  whiskers grown at 700 °C (Run 5). The solute concentration and the cooling rate were 0.5 mol-% and 5 °C h<sup>-1</sup>, respectively.

Table 1. Typical growth conditions of the  $\text{Na}_2\text{Ti}_6\text{O}_{13}$  whiskers and their average sizes.

Run	Solute conc. / mol-%	Holding temp. / °C	Cooling rate / °C h <sup>-1</sup>	Average length / μm	Average width / μm	Average aspect ratio
1	0.5	1100	5	24.2	0.8	30.3
2	0.5	1000	5	12.9	0.35	36.9
3	0.5	900	5	5.6	0.26	21.5
4	0.5	800	5	4.4	0.25	17.6
5	0.5	700	5	3.5	0.15	23.3
6	0.5	600	5	—	—	—
7	20	1100	5	7.8	0.58	13.4
8	20	1000	5	5.8	0.38	15.3
9	20	900	5	4.6	0.29	15.9
10	20	800	5	3.9	0.19	20.5
11	20	700	5	—	—	—
12	0.5	1000	>120000	11	0.43	25.6
13	0.5	900	>120000	4.6	0.25	18.4
14	0.5	800	>120000	3.8	0.16	23.8
15	0.5	700	>120000	—	—	—

results, the formation of highly crystalline, single-phase  $\text{Na}_2\text{Ti}_6\text{O}_{13}$  whiskers with high average aspect ratios was successfully grown at a relatively low temperature of 700 °C.

In order to fabricate whiskers with smaller sizes for a larger specific surface area, the crystals were first grown at a higher solute concentration of 20 mol-% or with a cooling rate >120000 °C h<sup>-1</sup> (water quenching). Figure 4a depicts the FESEM image of crystals grown at a solute concentration of 20 mol-%. In this case, the holding temperature and cooling rate were 700 °C and 5 °C h<sup>-1</sup>, respectively. The crystals exhibit 1D and plate-like structures, and a bulk-like structure due to remaining unreacted raw material. By contrast, well-developed, unique, and idiomorphic whiskers can clearly be observed in Figure 4b (at 800 °C, Run 10). The aspect ratio of the whiskers was about 20.5 ( $L_{\text{av}} = 3.9 \mu\text{m}$  and  $W_{\text{av}} = 0.19 \mu\text{m}$ ), and the size was larger than

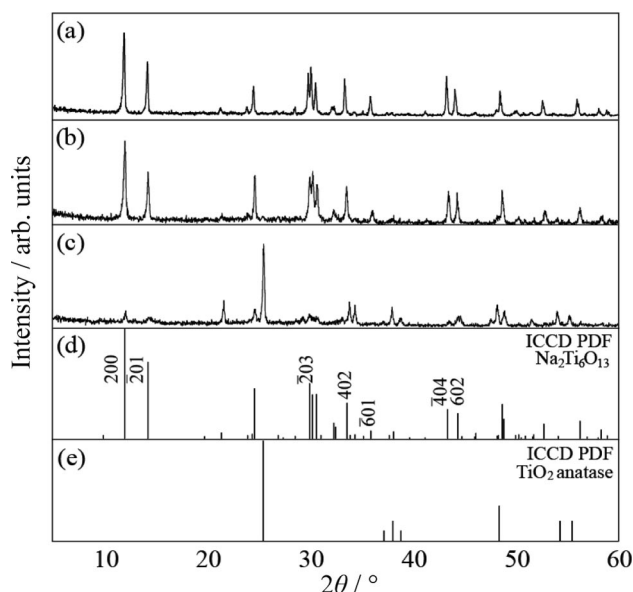


Figure 3. XRD patterns (Cu- $K_{\alpha}$ ) of grown products at (a) 1000 °C (Run 2), (b) 700 °C (Run 5), and (c) 600 °C (Run 6) and ICCD PDF of (d)  $\text{Na}_2\text{Ti}_6\text{O}_{13}$ <sup>[16]</sup> and (e)  $\text{TiO}_2$ .<sup>[17]</sup>

that of whiskers grown at 700 °C and 0.5 mol-% (Run 5); however, the whiskers grown at a solute concentration of 20 mol-% (Runs 7–10) were smaller than those at 0.5 mol-% (Runs 1–5), as shown Table 1. In addition, Figure 4c shows the FESEM image of crystals grown at a cooling rate of  $>120000\text{ °C h}^{-1}$ . The holding temperature and the solute concentration were 700 °C and 0.5 mol-%, respectively. These crystals exhibit whiskers and bulk-like structures. In contrast, well-developed, idiomorphic whiskers can clearly be observed in Figure 4d (at 800 °C, Run 14). The aspect ratio of the whiskers was about 23.8 ( $L_{\text{av}} = 3.8\text{ }\mu\text{m}$  and  $W_{\text{av}} = 0.16\text{ }\mu\text{m}$ ), and the size was larger than that of the whiskers grown at 700 °C and  $5\text{ °C h}^{-1}$  (Run 5); however, the whiskers grown at a cooling rate of  $>120000\text{ °C h}^{-1}$  (Runs 12–14) were smaller than those at  $5\text{ °C h}^{-1}$  (Runs 2–4), as shown in Table 1.

Figure 5 depicts the XRD profiles of the crystals grown from a solute concentration of 20 mol-% or with a cooling rate of  $>120000\text{ °C h}^{-1}$ . Figure 5a,b depicts XRD profiles of crystals grown at temperatures of 700 (Run 11) and 800 °C (Run 10), and at a solute concentration of 20 mol-% and a cooling rate of  $5\text{ °C h}^{-1}$ . Most of the diffraction peaks depicted in Figure 5a correspond to the powder diffraction patterns of  $\text{Na}_2\text{Ti}_6\text{O}_{13}$  (Figure 5e); however, the characteristic peak of  $\text{TiO}_2$  between 25 and 26° can be observed. Therefore, this diffraction patterns indicates that the bulk-like structure (Figure 4a) was a byproduct of  $\text{TiO}_2$ . By contrast, the whiskers grown at 800 °C (Run 10) were identified as  $\text{Na}_2\text{Ti}_6\text{O}_{13}$  by their powder XRD patterns in Figure 5b. The formation of highly crystalline  $\text{Na}_2\text{Ti}_6\text{O}_{13}$  whiskers with a single phase was demonstrated because the diffraction patterns attributed to byproducts were not observed. The XRD pattern for the oriented whiskers indicates that the diffraction intensities of the (200), ( $\bar{2}01$ ),

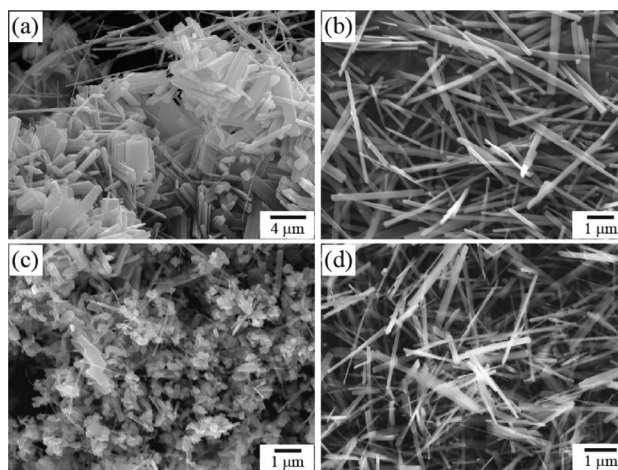


Figure 4. The effect of solute concentration and cooling rate on the formation of  $\text{Na}_2\text{Ti}_6\text{O}_{13}$  whiskers. SEM images show the products grown with a solute concentration of 20 mol-%, a cooling rate of  $5\text{ °C h}^{-1}$ , holding temperatures of (a) 700 °C (Run 11) and (b) 800 °C (Run 10). In addition, the products were grown with a solute concentration of 0.5 mol-%, a cooling rate of  $>120000\text{ °C h}^{-1}$ , and holding temperatures of (c) 700 °C (Run 15) and (d) 800 °C (Run 14).

( $\bar{2}03$ ), (402), ( $\bar{6}01$ ), ( $\bar{4}04$ ), and (602) planes were dominant. Figure 5c,d shows the XRD profiles of the crystals grown at temperatures of 700 (Run 15) and 800 °C (Run 14) at a cooling rate of  $>120000\text{ °C h}^{-1}$  and with a solute concentration of 5 mol-%. The crystals grown at 700 °C exhibit the

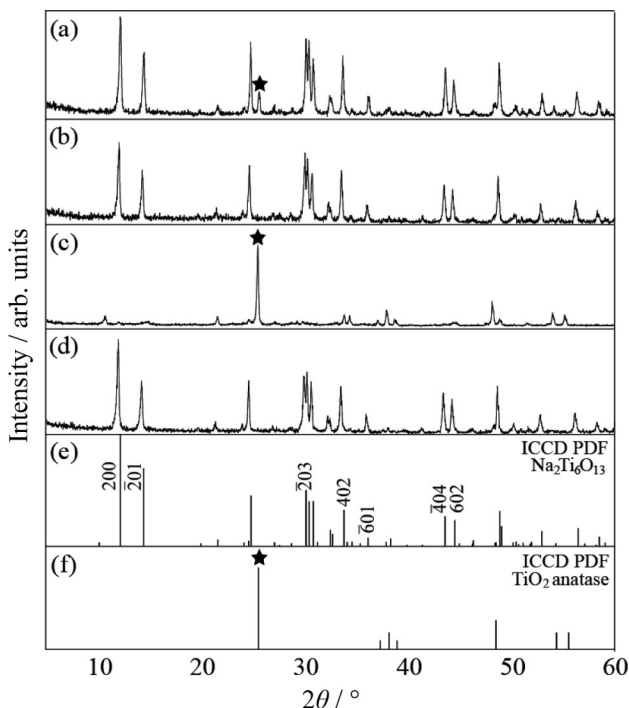


Figure 5. XRD patterns (Cu- $K_{\alpha}$ ) of products grown with a solute concentration of 20 mol-%, a cooling rate of  $5\text{ °C h}^{-1}$ , and holding temperatures of (a) 700 °C (Run 11) and (b) 800 °C (Run 10), and products grown at a solute concentration of 0.5 mol-%, a cooling rate of  $>120000\text{ °C h}^{-1}$ , and holding temperatures of (c) 700 °C (Run 15) and (d) 800 °C (Run 14).



coexistence of  $\text{Na}_2\text{Ti}_6\text{O}_{13}$  and  $\text{TiO}_2$ . The diffraction pattern (Figure 5c) indicates that the bulk-like structure (Figure 4c) was a byproduct (or unreacted raw material) of  $\text{TiO}_2$ . By contrast, the whiskers grown at 800 °C (Run 14) were identified as  $\text{Na}_2\text{Ti}_6\text{O}_{13}$  by their powder XRD patterns in Figure 5d. The diffraction patterns of the crystals attributed to byproducts cannot be observed. Therefore, the formation of highly crystalline, single-phase  $\text{Na}_2\text{Ti}_6\text{O}_{13}$  whiskers can be confirmed in Figure 5d.

Figure 6a,b depicts a bright-field TEM image and the corresponding selected area diffraction pattern (SAED) of a typical  $\text{Na}_2\text{Ti}_6\text{O}_{13}$  whisker (holding temperature = 800 °C, solute concentration = 20 mol-%, cooling rate = 5 °C h<sup>-1</sup>, Run 10). The bright-field TEM image demonstrates that the whisker has a well-formed, hexagonal-cylindrical shape, and the surface is very flat. The diffraction spots in the SAED pattern were confirmed to agree with  $\text{Na}_2\text{Ti}_6\text{O}_{13}$ . In addition, the SAED indicated that the interplanar spacings of the whisker are  $d_{020} = 0.188$  nm and  $d_{202} = 0.362$  nm, which agree well with those obtained in a previous study. Because the incident electron beam is parallel to the  $[\bar{1}01]$  direction, the lattice parameter  $a$  cannot be measured by using only this incident beam. The lattice image obtained from a  $\text{Na}_2\text{Ti}_6\text{O}_{13}$  whisker is shown in Figure 6c, taken with the incident beam along the  $[\bar{1}01]$  direction. The whisker was of very good crystallinity because no defects were observed in this image. From these SEM, XRD, and TEM results, we can conclude that the elongated direction clearly corresponded to the  $\langle 010 \rangle$  directions. Considering the lattice pa-

rameters, it seems reasonable to elongate along the  $\langle 010 \rangle$  directions, which was the same result obtained in our previous study.

The UV/Vis diffuse reflectance spectrum of the  $\text{Na}_2\text{Ti}_6\text{O}_{13}$  whiskers (holding temperature = 800 °C, solute concentration = 20 mol-%, cooling rate = 5 °C h<sup>-1</sup>, Run 10) is shown in Figure 7a. The UV/Vis diffuse reflectance spectra of the  $\text{Na}_2\text{Ti}_6\text{O}_{13}$  whiskers grown in this study are essentially the same. The spectra show the onset wavelength of absorption at around 365 nm and a maximum at around 315–325 nm. The calculated band gap was about 3.4 eV. From these spectra, there is a fair possibility that all of the  $\text{Na}_2\text{Ti}_6\text{O}_{13}$  whiskers reveal photocatalytic properties under UV (<360 nm) light irradiation. Furthermore, the photocatalytic characteristics of the  $\text{Na}_2\text{Ti}_6\text{O}_{13}$  whiskers were investigated by the photodecolorization of organic dyes (methyl orange), as shown in Figure 7b. The  $\text{Na}_2\text{Ti}_6\text{O}_{13}$  whiskers acted efficiently as photocatalysts under black light lamp irradiation, and the characteristic colors of the organic dyes faded gradually due to their photocatalytic effect. In comparison to our previous study (whiskers grown at 1100 °C), the whiskers grown in this study exhibited many advantages as photocatalysts because they had a large specific surface area due to their smaller size. In addition, they also exhibited many advantages over photocatalytic  $\text{TiO}_2$  or polycrystalline  $\text{Na}_2\text{Ti}_6\text{O}_{13}$  produced by other methods because of their much higher crystallinity.

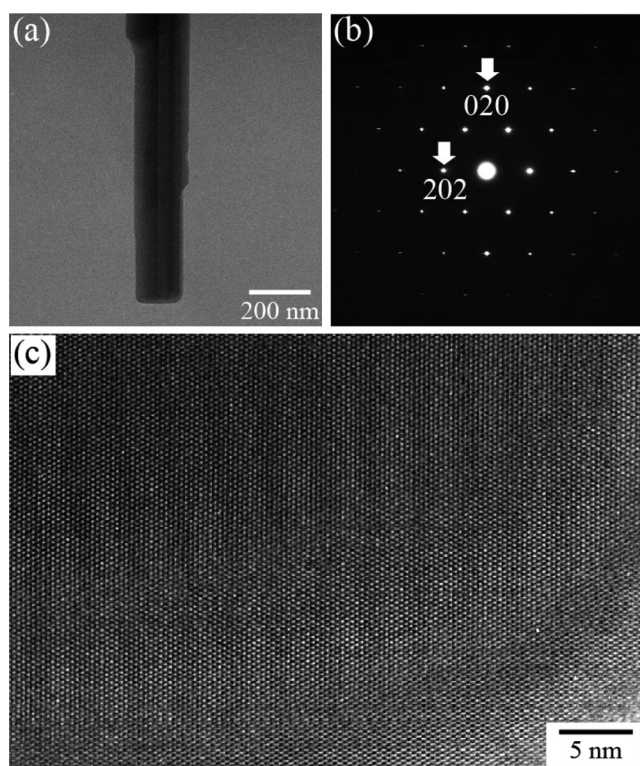


Figure 6. (a) Bright-field TEM micrograph, (b) selected area electron diffraction pattern, and (c) lattice image of a typical  $\text{Na}_2\text{Ti}_6\text{O}_{13}$  whisker.

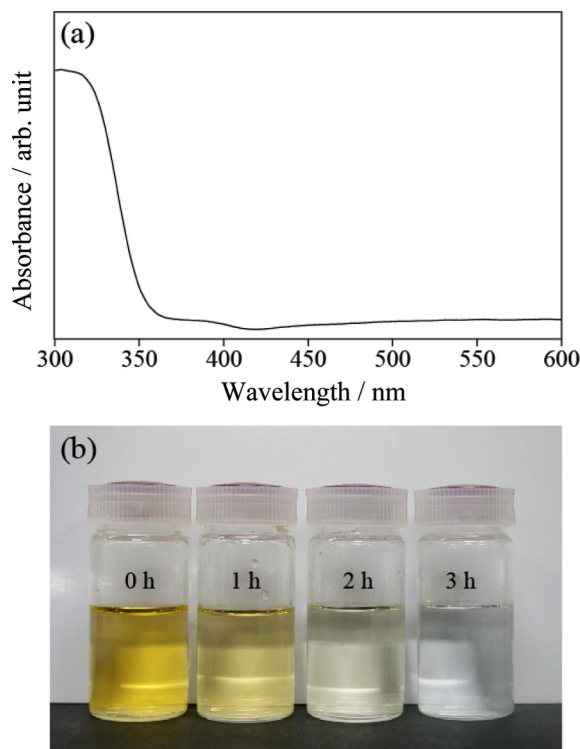


Figure 7. (a) UV/Vis light diffuse reflectance spectrum of a  $\text{Na}_2\text{Ti}_6\text{O}_{13}$  whisker (Run 10) and (b) photodecolorization of an organic dye (methyl orange) under black light lamp (the ray wavelength between 300 and 400 nm) irradiation for 0 to 3 h.

## Conclusions

High quality, well-developed, transparent, and colorless  $\text{Na}_2\text{Ti}_6\text{O}_{13}$  whiskers were successfully grown by the cooling of a NaCl flux at 700 to 1000 °C. Their basic form included a hexagonal rod with relatively smooth surfaces. The whiskers obtained at a relatively lower temperature of 700 °C exhibited the lowest sizes of up to  $3.5\text{ }\mu\text{m} \times 0.15\text{ }\mu\text{m}$ . Under the conditions of low temperature (600 °C), high solute concentration (20 mol-%), and rapid cooling rate ( $>120000\text{ }^\circ\text{C h}^{-1}$ , water quenching), both  $\text{Na}_2\text{Ti}_6\text{O}_{13}$  whiskers and  $\text{TiO}_2$  byproducts (or unreacted raw material) are formed. These whiskers exhibit a high crystallinity and hexagonal cylinder elongated in the  $\langle 010 \rangle$  directions. Furthermore, they acted efficiently as a photocatalyst under UV light irradiation, and the characteristic color of methyl orange solution faded by the photocatalytic effect. The formation of highly crystalline, active photocatalyst  $\text{Na}_2\text{Ti}_6\text{O}_{13}$  whiskers was confirmed from these results. Finally, we recognize that NaCl can adequately be used for the environmentally friendly growth of  $\text{Na}_2\text{Ti}_6\text{O}_{13}$  whiskers.

## Experimental Section

**Synthesis:**  $\text{Na}_2\text{Ti}_6\text{O}_{13}$  whiskers were easily grown by using a NaCl flux cooling method at a relatively low temperature ( $<1100\text{ }^\circ\text{C}$ ). Reagent-grade  $\text{Na}_2\text{CO}_3$  (Wako Pure Chemical Industries),  $\text{TiO}_2$  (anatase, Wako Pure Chemical Industries), and NaCl (Wako Pure Chemical Industries) were used for the growth of the  $\text{Na}_2\text{Ti}_6\text{O}_{13}$  whiskers. First, a stoichiometric mixture of  $\text{Na}_2\text{CO}_3$  and  $\text{TiO}_2$  powders (molar ratio  $\text{Na}_2\text{CO}_3/\text{TiO}_2 = 1:6$ ) and NaCl were respectively used as a solute and the flux. The typical growth conditions are given in Table 1. The solute concentration was fixed at 0.5 or 20 mol-% of the NaCl flux. These masses of the reagents were kept at approximately 20 g for all growth runs. Each of the mixtures was put into platinum crucibles of  $30\text{ cm}^3$  capacity. After the lids were loosely closed, the crucibles were placed in an electric furnace. The crucibles were heated to 600–1000 °C at a rate of  $45\text{ }^\circ\text{C h}^{-1}$  and held at this temperature for 10 h. After that, they were cooled to 500 °C at a rate of  $5\text{ }^\circ\text{C h}^{-1}$  (slow cooling) or  $>120000\text{ }^\circ\text{C h}^{-1}$  (water quenching). The cooling rate of  $5\text{ }^\circ\text{C h}^{-1}$  was controlled by the cooling program. The cooling rate of  $>120000\text{ }^\circ\text{C h}^{-1}$  was not able to be attained by the cooling program in the furnace. For  $>120000\text{ }^\circ\text{C h}^{-1}$ , after they were removed from the high-temperature furnace, the crucibles were immersed into water and cooled extremely rapidly. The cooling rate of  $>120000\text{ }^\circ\text{C h}^{-1}$  is an approximate estimated value. The crystal products were separated from the remaining flux in warm water.

**Characterization:** The obtained crystals were observed by use of an optical microscope and field-emission scanning electron microscope (FESEM, JEOL, JSM-7000F). Phases and elongated directions of the crystals were studied by X-ray diffraction (XRD, SHIMADZU, XRD-6000). The high-resolution transmission electron microscopy (HRTEM) and electron diffraction observations were carried out with JEM-2010 (JEOL) and JEM-2000EXII (JEOL) instruments operated at 200 kV to analyze the crystallinity and elongated direction of the grown crystals. The presence of impuri-

ties from the NaCl flux and platinum crucible was also observed. The length ( $L$ , parallel to the  $\langle 010 \rangle$  directions) and width ( $W$ , perpendicular to the  $\langle 010 \rangle$  directions) of relatively large  $\text{Na}_2\text{Ti}_6\text{O}_{13}$  whiskers (100 samples) were measured by SEM observation, and their average sizes ( $L_{\text{av}}$  and  $W_{\text{av}}$ ) and aspect ratios ( $L_{\text{av}}/W_{\text{av}}$ ) were calculated for each growth run. The ultraviolet/visible (UV/Vis) light diffuse reflectance spectra of the grown crystals were obtained with a spectrophotometer (SHIMADZU, UV3150). To simply examine its photocatalytic property, photodecolorization examination of methyl orange solution ( $\text{C}_{14}\text{H}_{14}\text{N}_3\text{NaO}_3\text{S}$ , 0.1 wt.-%, Wako Pure Chemical Industries) of 100 mL was carried out. The  $\text{Na}_2\text{Ti}_6\text{O}_{13}$  whiskers of 0.5 g grown at 800 °C (Run 4) were used as photocatalyst. After irradiating black light lamp (the ray wavelength between 300 and 400 nm, 15 W) for 1–3 h, the color of the organic dyes was investigated.

**Supporting Information** (see footnote on the first page of this article): Low- and high-magnification FESEM images of the products grown at 700 °C without adding a NaCl flux.

## Acknowledgments

This research was partially supported by Industrial Technology Research Grant Program in 2009 from New Energy and Industrial Technology Development Organization (NEDO) of Japan (No. 09A18002a) and a Grant-in-Aid from the Ministry of Education, Culture, Sports, Science and Technology, Japan (No. 20350093). Part of this work was supported by the Steel Industry Foundation for the Advancement of Environmental Protection Technology (2007–2008).

- [1] L. M. Viculis, J. J. Mack, R. B. Kaner, *Science* **2003**, 299, 1361.
- [2] Y. Ding, Y. Wan, Y. L. Min, W. Zhang, S. H. Yu, *Inorg. Chem.* **2008**, 47, 7813–7823.
- [3] K. Teshima, K. Yubuta, T. Shimodaira, T. Suzuki, M. Endo, T. Shishido, S. Oishi, *Cryst. Growth Des.* **2008**, 8, 465–469.
- [4] K. Teshima, K. Yubuta, S. Sugiura, T. Suzuki, T. Shishido, S. Oishi, *Bull. Chem. Soc. Jpn.* **2006**, 79, 1725–1728.
- [5] M. Yada, Y. Inoue, M. Uota, T. Torikai, T. Watari, I. Noda, T. Hotokebuchi, *Langmuir* **2007**, 23, 2815–2823.
- [6] X. Sun, X. Cher, Y. Li, *Inorg. Chem.* **2002**, 41, 4996–4998.
- [7] D. Kuang, J. Brillet, P. Chen, M. Takata, S. Uchida, H. Miura, K. Sumioka, S. M. Zakeeruddin, M. Grätzel, *ACS Nano* **2008**, 2, 1113–1116.
- [8] X. Peng, L. Manna, W. Yang, J. Wickham, E. Scher, A. Kadavanich, A. P. Alivisatos, *Nature* **2000**, 404, 59–61.
- [9] Y. Mao, S. S. Wong, *J. Am. Chem. Soc.* **2006**, 128, 8217–8226.
- [10] Y. D. Li, X. L. Li, R. R. He, J. Zhu, Z. X. Deng, *J. Am. Chem. Soc.* **2002**, 124, 1411–1416.
- [11] F. Amano, K. Nogami, R. Abe, B. Ohtani, *J. Phys. Chem. C* **2008**, 112, 9320–9326.
- [12] S. H. Lee, K. Teshima, Y. Niina, S. Suzuki, K. Yubuta, T. Shishido, M. Endo, S. Oishi, *CrystEngComm* **2009**, 11, 2326–2331.
- [13] C. C. Tsai, H. Teng, *Chem. Mater.* **2006**, 18, 367–373.
- [14] J. Ramirez-Salgado, E. Djurado, P. Fabry, *J. Eur. Ceram. Soc.* **2004**, 24, 2477–2483.
- [15] Y. Inoue, T. Kubokawa, K. Sato, *J. Chem. Soc., Chem. Commun.* **1990**, 1298–1299.
- [16] ICDD PDF 73-1398.
- [17] ICDD PDF 21-1272.

Received: December 4, 2009  
Published Online: May 19, 2010